PRJ, Vol. 8 (January 1996); P. 1–11, 24 FIGS. 4 TABLES.

Equation of State Applieation to Predict MMC and MMP for Raguba Oil Field, Libya

A.H. Al-Khafaji*, M.M. Alswieh*, S.T. Abuzbeda*, and S.O. Alabani*

تطبيق معادلة الحالة للتنبؤ بالتركيب الإمتزاجي الأدنى والضغط الإمتزاجي الأدنى لنفط حقل الراقوبة ، ليبيا

علي حبيب الخفاجي ، محمد مسعود السويح ، صلاح الدين أبو زبيدة و سالم عمران العباني

تم في هذا البحث تمثيل عينتين من النفط المكمني بواسطة معادلة الحالة EOS لـ (بنك روبنسن) واستعمال منظومة (CMG-Prop). لقد طورت خصائص معادلة الحالة لكل من العينتين النفطيتين بهدف استنباط تراكيب المحاليل المثلى. أي الحد الأدنى للتركيب الإمتزاجي (MMC) لخليط محاليل الغاز السائل — الغاز الجاف والضغط الإمتزاجي الأدنى (MMP) لغاز ثاني أكسيد الكربون في الإفاضة المتجانسة. وجرى تنعيم عوامل معادلة الحالة لكي تتوافق مع البيانات الإختبارية للضغط والحجم والحرارة بالإضافة إلى اللزوجة لكلا العينتين النفطية. وعليه تم الحصول على الشكل البياني الطوري. والشكل الثلاثي الإجمالي والشكل لعلاقة الضغط — التركيب لكلا العينتين النفطية الملامسة مع تراكيب مختلفة من محاليل الغاز السائل — الغاز الجاف وكذلك غاز ثاني أوكسيد الكربون وفي درجة حرارة المكمن النفطي 206° ف.

وجد بأن الدفع المكثف هو الميكانيكية الرئيسة في استخراج النفط لكلا العينتين عند التركيب الإمتزاجي الأدنى للمحلول ، وحصل التجانس لهاتين العينتين مع ثاني أكسيد الكربون عند ضغط يعتبر عال نسبياً.

لقد ساعدت المعلومات أعلاه على تصميم اختبارات الإمتزاجية باستعمال الأنبوب الرفيع وكذلك اختبارات عملية الإنتفاخ.

Abstract *In this investigation, Peng-Robinson equation of state (EOS) modelling for two recombined reservoir oil samples is represented using the Computer Modelling Group (CMG PROP) software. EOS characterizations for these oils were developed to predict optimum solvent compositions-minimum miscibility composition (MMC) for LPG-Dry Gas mixtures, and minimum miscibility pressure (MMP) for CO_2 in miscible flooding. EOS parameters were tuned to match the experimental PVT data besides viscosity data for both oils. Accordingly, phase diagrams, pseudoternary diagrams and pressure-composition diagrams for both oils in contact with several LPG-Dry Gas compositions and/or CO_2 were generated at reservoir temperature of 206 °F.*

It was found that the main mechanism of oil recovery is a condensing drive for both oils at minimum miscibility composition. Miscibility of these oils with CO_2 was achieved at a pressure considerably high. These foundings were used to help design slim tube experiments as well as swelling experiments.

INTRODUCTION

Study of miscibility of different solvents and gases with reservoir oil is one of the most important processes to enhance oil recovery. Literatures on theoretical studies,[1,2,3,4,5] experimental laboratory investigations[6,7,8,9] and field applications[10,11] of miscibility are available. Miscibility is achieved at certain conditions of pressure and temperature depending on the composition of both the reservoir oil and the injected gases or solvents. There are generally two types of miscible processes, the first contact miscible (FCM),

* Petroleum Research Centre, P.O. Box 6431, Tripoli, G.S.P.L.A.J.

where solvent (LPG) mix directly with reservoir oil in all proportions and their mixtures always remain in a single phase. The second process is the multiple contact miscible (MCM) process-dynamic miscibility processes, where gases or solvents are not directly miscible with reservoir oil, but under a appropriate conditions of pressure, temperature and oil-gas or oil-solvent compositions, *in-situ* miscibility could be achieved through repeated contacts of the injected material with reservoir oil. The MCM is of three kinds: the vaporizing, the condensing and condensing/vaporizing miscible processes.

In the present investigation, equation of state (EOS) characterizations of two recombined oils (1800R & 2030R) were developed in order to predict the minimum miscibility composition (MMC) for rich-gas and minimum miscibility pressure (MMP) for CO_2 in miscible flooding processes. Peng-Robinson[12,13] cubic equation of state was applied for both oils. Equation of state parameters were tuned to match all available experimental data for these oils. Then, pseudoternary diagrams and pressure-composition diagrams for the oils in contact with several rich gas compositions and/or CO_2 were generated to figure out the mechanisms of oil recovery and the optimum compositions and pressures for gas injection with rich gas and/or CO_2. This information was used to help design slim tube experiments as well as swelling experiments. Once these experiments were completed then the EOS characterization can be revised and compositional simulation could be undertaken.

EXPERIMENTAL DATA

Experimental data were available for two recombined oils 1800R and 2030R with bubble point pressures of 1800 psia and 2030 psia respectively.[14,15] These oils were directly recombined from the separator gas and oil at a specific gas oil ratio (GOR). The two oils are essentially the same except that 2030R has a greater amount of solution gas. Thus, it should be possible to characterize the C_{7+} for the oils with the same pseudocomponents. For each oil the experimental data available include bubble point pressure-flash liberation, direct flash, recombination of separator oil and gas and differential liberation data.

SPLITTING OF C_{7+}

Since both oils are derived from the same source except for a difference in the amount of the solution gas, it should be possible to use one set of plus fraction components for both oils. In order to split the plus fraction of the two oils the molecular weight and specific gravity of the plus fraction are required. The molecular weight of the plus fraction can be calculated from the extended chromatographic analysis. The molecular weight of the plus fraction for both oils 1800R and 2030R were about 155. Specific gravity of the plus fraction for oil 1800R was estimated to be about 0.85 by using specific gravity of the stock tank oil that was 0.8201. This information was used to split the plus fraction into two pseudocomponents. The properties of the two pseudocomponents. The properties of the two pseudocomponents are shown on Table 1 for oil sample 1800R and 2030R. It was found that two pseudocomponents were adequate to model these oils because of the large amount of components present between C_7 and C_{13}.

TUNING OF EOS PARAMETERS

In order to assure the accuracy of EOS predictions of miscibility conditions for these two oils, the EOS parameters must first be tuned to match experimental data, then a more reliable analysis of recovery mechanism and miscibility conditions may be made. The tuning is accomplished using the regression option in CMG PROP. The regression variables are critical pressure and temperature, the volume shifts of methane, and the C_{7+} components. Also, the binary interaction coefficient exponent and the molecular weights of the C_{7+} components were used as regression variables as represented in Table 1. These variables were adjusted to match the experimental data for both oils including the bubble point pressures, the flash liberation data, the differential liberation data, and the separator flash data. A high weight was given to matching the bubble point pressure data since the match of all the other experiments depended on having an accurate bubble point pressure. After several different regression runs, a good match of the experimental data was achieved. The final values of the regression variables and the match of the experimental data are shown on Tables 3 & 4. An acceptable match of the results for both oils was achieved (Figs. 1–13).

GENERATION OF PHASE DIAGRAMS AND DETERMINATION OF MISCIBILITY CONDITIONS

Using the tuned EOS parameters, the conditions for miscibility and the mechanism of oil recovery can be analyzed using multiple contact ternary diagrams as well as pressure-composition and pressure-temperature diagrams. First, the pressure-temperature diagrams were generated for both oils (Fig. 14). These diagrams are consistent with the typical diagrams for black oils with the reservoir temperature much lower

Table 1. EOS components properties for reservoir oils 1800R and 2030R at 206 F, Raguba oil field, Well No. E40.

Component	*MW*	*Critical Pressure*	*Critical Temperature*	*Critical Volume*	*Acentric Factor*	*Volume Shift*	*Interaction Coefficient* Hydrocarbon and*		*Critical Volume***		*Oil Composition Mole Fraction*	
									1800R	*2030R*		
		Pc, Atm.	*Tc, K*	*Vc, l/gmol*	*AC*		*N2*	*CO2*	*Vc, l/gmol*	*Vc, l/gmol*	*1800R*	*2030R*
N2	28.01	33.50	126.20	8.950E-02	4.000E-02	−1.284E-01		−2.08E-02	8.950E-02	8.950E-02	2.08E-03	2.57E-03
CO_2	44.01	72.80	304.20	9.400E-02	2.250E-01	−9.435E-02	−2.08E-02		9.400E-02	9.400E-02	5.89E-03	6.34E-03
C1	16.04	46.73	164.73	9.900E-02	8.000E-03	−1.237E-01	3.10E-02	1.03E-01	9.900E-02	9.900E-02	2.08E-01	2.31E-01
C2	30.07	48.20	305.40	1.480E-01	9.800E-02	−1.021E-01	4.20E-02	1.30E-01	1.480E-01	1.480E-01	7.53E-02	7.80E-02
C3	44.10	41.90	369.80	2.030E-01	1.520E-01	−7.330E-02	9.10E-02	1.35E-01	2.030E-01	2.030E-01	7.53E-02	7.50E-02
iC4	58.12	36.00	408.10	2.630E-01	1.760E-01	−5.707E-02	9.50E-02	1.30E-01	2.630E-01	2.630E-01	2.49E-02	2.44E-02
nC4	58.12	37.50	425.20	2.550E-01	1.930E-01	−5.706E-02	9.50E-02	1.30E-01	2.550E-01	2.550E-01	6.85E-02	6.65E-02
iC5	72.15	33.40	460.40	3.060E-01	2.270E-01	−3.446E-02	9.50E-02	1.25E-01	3.060E-01	3.060E-01	3.46E-02	3.34E-02
nC5	72.15	33.30	469.60	3.040E-01	2.510E-01	−3.443E-02	9.50E-02	1.25E-01	3.040E-01	3.040E-01	3.80E-02	3.66E-02
FC6	86.00	30.26	563.61	3.440E-01	2.750E-01	−4.227E-03	1.20E-01	1.50E-01	3.440E-01	3.440E-01	5.37E-02	5.15E-02
C7–C13	138.85	23.72	706.99	4.755E-01	3.403E-01	2.258E-01	1.20E-01	1.50E-01	5.706E-01	5.706E-01	3.20E-01	3.12E-01
C14+	301.90	14.84	956.18	8.384E-01	6.436E-01	8.824E-02	1.20E-01	1.50E-01	8.569E-01	6.707E-01	9.24E-02	8.21E-02

OMEGA = 0.45723553 in the EOS
OMEGB = 0.07796074 in the EOS
MIXVC = 0.82733389, exponent coefficient used in viscosity calculations, for Oil 1800R, (see Appendix A)
MIXVC = 0.80000000, exponent coefficient used in viscosity calculations, for Oil 2030R, (see Appendix A)
PVC3 = 2.000, binary interaction coefficient exponent for hydrocarbon–hydrocarbon component pairs
*binary interaction coefficient for hydrocarbon–non-hydrocarbon component pairs
**Component pseudo-critical volume used to compute the mixture critical volume used in viscosity calculations

than the critical temperature. Next, series of pseudoternary diagrams were generated for oil 1800R at 1850 psia contacted by various solvents made up by blending LPG with dry gas in different molar ratios (from 30% to 60% LPG). The compositions of these various solvents, LPG and dry gas are represented in Table 2. Figure 15 shows the ternary diagram for oil 1800R contacted by solvent with LPG ratios of 55%. From this diagram, evidently miscibility is achieved when the solvent composition is around 55% LPG or greater. The pressure-composition diagrams for oil 1800R with different solvents is shown in Fig. 16. From this figure, it is evident that until the LPG ratio is 50% the principal mechanism of recovery will be via vaporizing mechanism. However, at higher LPG ratios, the mechanism becomes principally a condensing mechanism. Thus, miscibility is achieved with a solvent with LPG of 55% or greater by a condensing mechanism where the liquid phase becomes enriched with intermediates to the point that it becomes miscible with the injected gas.

The pseudoternary diagrams for oil 2030R at pressure of 2100 psia show that miscibility is achieved for a solvent with 50% LPG or greater (Fig. 17). To analyze the mechanism of recovery we examine the pressure composition diagrams for these systems (Fig. 18) just as we did for oil 1800R. From this diagram, it appears that up to 40% LPG in the solvent of the principal mechanism of recovery is a vaporizing mechanism but for more LPG in solvent the mechanism becomes primarily a condensing mechanism.

Ternary diagrams[16,17] for oil 1800R contacted with CO_2 at several different pressures were generated to determine the miscibility pressure for this oil with CO_2. The ternary diagram for pressures of 1850, 3000, and 4400 psia is shown in Fig. 19. For all these

Table 2. Solvents composition of the blended LPG/Dry gas samples.

Component	*Dry Gas*	*0.40 LPG**	*0.45 LPG*	*0.5 LPG*	*0.55 LPG*	*0.6 LPG*	*LPG*
	Mole%	*Mole%*	*Mole%*	*Mole%*	*Mole%*	*Mole%*	*Mole%*
N2	1.358	0.815	0.747	0.679	0.611	0.543	
CO_2							
C1	86.419	51.851	47.530	43.210	38.889	34.568	
C2	8.354	6.000	5.706	5.412	5.117	4.823	2.469
C3	2.831	13.560	14.901	16.243	17.584	18.925	29.654
IC4	0.389	9.444	10.576	11.708	12.839	13.971	23.026
NC4	0.649	18.330	20.540	22.750	24.960	27.170	44.850

*0.40 LPG: Molar Ratio of 0.40 LPG to 0.60 Dry Gas.

Table 3. Comparison of experimental data with EOS predicted values before and after regression analyses, reservoir oil sample of Pb = 1800 psia at 206F, Raguba oil field, Well No. E40.

Exper. Processes	*Data Type*	*Pressure psig*	*Exper. Values*	*Predicted Values*		*Error* Reduction*	*Error** After*	*Weight Factor*
				Before	*After*			
	Pb Psia	—	1800	1378.9	1805.8	0.2307	0.0032	200
Differential	Solution	1785	674.50	1358.20	716.95	0.9508	0.0629	12
Liberation	GOR	1500	588.60	1358.20	642.62	1.2158	0.0918	12
	Scf/bbl	1200	494.84	1253.20	567.63	1.3855	0.1471	12
		900	400.51	1067.60	493.17	1.4344	0.2314	12
		600	309.93	886.29	416.43	1.5160	0.3436	12
		300	206.31	687.19	325.85	1.7515	0.5794	12
		0	0.00	0.00	0.00	0.0000	0.0000	12
	Liberated	1785		0.844	0.897	0.0526	0.1029	0
	Gases	1500	0.813	0.836	0.900	−0.0778	0.1066	2.5
	Z-factor	1200	0.842	0.853	0.904	−0.0611	0.0741	2.5
		900	0.856	0.871	0.911	−0.0468	0.0644	2.5
		600	0.886	0.892	0.920	−0.0310	0.0380	2.5
		300	0.917	0.917	0.930	−0.0144	0.0145	2.5
		0	1.000	0.982	0.986	0.0039	0.0137	2.5
	Liquid	1785	0.675	0.772	0.669	0.1356	0.0087	4
	Densities	1500	0.685	0.776	0.676	0.1184	0.0139	4
	g/cc	1200	0.696	0.785	0.682	0.1084	0.0196	4
		900	0.708	0.809	0.690	0.1171	0.0259	4
		600	0.720	0.836	0.698	0.1295	0.0309	4
		300	0.736	0.868	0.708	0.1415	0.0377	4
		0	0.750	1.009	0.755	0.3386	0.0060	4
	Oil FVF	1785	1.457	2.005	1.495	0.3499	0.0259	2.5
	Bbl/stb	1500	1.414	1.997	1.462	0.3779	0.0340	2.5
		1200	1.367	1.948	1.429	0.3802	0.0450	2.5
		900	1.320	1.848	1.394	0.3436	0.0562	2.5
		600	1.274	1.747	1.357	0.3062	0.0652	2.5
		300	1.215	1.629	1.308	0.2643	0.0766	2.5
		0	1.080	1.077	1.051	−0.0239	0.0266	2.5
Direct	API	0	41.039	6.333	50.074	0.6255	0.2202	0.1
Flash	FVF	0	1.413	1.593	1.362	0.0914	0.0358	0.1
Liberation	GOR	0	762.40	821.58	547.25	−0.2046	0.2822	0.1
Constant	Relative	5000	0.9596	0.9283	0.9555	0.0284	0.0043	1
Composition	Oil	4000	0.9697	0.9429	0.9667	0.0245	0.0031	1
Liberation	Volume	3000	0.9817	0.9607	0.9800	0.0197	0.0017	1
		2500	0.9885	0.9711	0.9878	0.0169	0.0007	1
		2000	0.9961	0.9829	0.9964	0.0130	0.0003	1
		1900	0.9970	0.9855	0.9982	0.0104	0.0012	1
		1850	0.9977	0.9868	0.9992	0.0095	0.0015	1
		1785	1.0000	0.9885	1.0045	0.0071	0.0045	1
		1770	1.0058	0.9889	1.0078	0.0149	0.0020	1
		1700	1.0207	0.9908	1.0242	0.0259	0.0035	1
		1600	1.0461	0.9936	1.0509	0.0456	0.0046	1
		1500	1.0773	0.9964	1.0822	0.0706	0.0045	1
		1300	1.1649	1.0419	1.1630	0.1039	0.0016	1
		1000	1.4097	1.2838	1.3611	0.0549	0.0345	1
		700	1.9991	1.8016	1.7733	−0.0142	0.1130	1
Reservoir	Oil	5000	0.8522	0.1466	0.8720	0.8048	0.0232	1
Oil	Viscosity	4500	0.8235	0.1427	0.8382	0.8089	0.0179	1
Viscosity	cp	4000	0.7948	0.1386	0.8037	0.8144	0.0112	1
Meas.		3500	0.7661	0.1344	0.7685	0.8214	0.0032	1
		3000	0.7369	0.1301	0.7325	0.8176	0.0060	1
		2500	0.7081	0.1256	0.6957	0.8051	0.0176	1
		2200	0.6909	0.1228	0.6731	0.7964	0.0258	1
		2100	0.6852	0.1219	0.6655	0.7933	0.0288	1
		2050	0.6822	0.1214	0.6617	0.7919	0.0301	1
		2015	0.6804	0.1211	0.6590	0.7906	0.0315	1
		1785	0.6682	0.1189	0.6413	0.7818	0.0402	1
		1500	0.6725	0.1204	0.6730	0.8202	0.0008	1
		1200	0.6813	0.1219	0.7094	0.7798	0.0412	1
		900	0.6916	0.1235	0.7513	0.7353	0.0862	1
		600	0.7469	0.1250	0.8016	0.7594	0.0732	1
		300	0.9688	0.1268	0.8717	0.7689	0.1002	1
		0	1.2089	0.1294	1.1963	0.8825	0.0104	1

*Error Reduction = Error before Regression − Error after Regression

**Error after = (Experimental − Calculated)/Experimental

Table 4. Comparison of experimental data with EOS predicted values before and after regression analyses, reservoir oil sample of Pb = 2030 psia at 206F, Raguba oil field, Well No. E40.

Exper. Processes	*Data Type*	*Pressure psig*	*Exper. Values*	*Predicted Values*		*Error* Reduction*	*Error** After*	*Weight Factor*
				Before	*After*			
Differential Liberation	Pb Psia	—	2030	1534.7	2027.8	0.2429	0.0011	200
	Solution	2015	780.26	1511.40	800.34	0.9113	0.0257	12
	GOR	1800	703.64	1511.40	742.40	1.0928	0.0551	12
	Scf/bbl	1500	603.16	1497.50	662.79	1.3839	0.0989	12
		1200	508.23	1292.90	585.12	1.3926	0.1513	12
		900	414.91	1100.70	508.09	1.4282	0.2246	12
		600	326.62	913.24	428.75	1.4833	0.3127	12
		300	215.63	707.85	335.07	1.7288	0.5539	12
		0	0.00	0.00	0.00	0.0000	0.0000	12
	Liberated	2015		0.837	0.896	0.0592	0.1041	0
	Gases	1800	0.859	0.826	0.896	−0.0049	0.0436	2.5
	Z-factor	1500	0.851	0.838	0.899	−0.0408	0.0566	2.5
		1200	0.894	0.853	0.904	0.0352	0.0110	2.5
		900	0.919	0.871	0.911	0.0433	0.0092	2.5
		600	0.944	0.892	0.919	0.0288	0.0264	2.5
		300	0.970	0.917	0.930	0.0136	0.0413	2.5
		0		0.982	0.986	0.0040	0.0137	0
	Liquid	2015	0.648	0.756	0.662	0.1453	0.0221	4
	Densities	1800	0.656	0.763	0.667	0.1464	0.0167	4
	g/cc	1500	0.666	0.758	0.674	0.1264	0.0117	4
		1200	0.676	0.782	0.681	0.1491	0.0072	4
		900	0.686	0.806	0.688	0.1720	0.0035	4
		600	0.697	0.833	0.697	0.1949	0.0004	4
		300	0.710	0.866	0.708	0.2165	0.0035	4
		0	0.749	1.009	0.755	0.3395	0.0081	4
	Oil FVF	2015	1.570	2.097	1.537	0.3148	0.0208	2.5
	Bbl/stb	1800	1.527	2.079	1.512	0.3517	0.0098	2.5
		1500	1.478	2.090	1.477	0.4130	0.0008	2.5
		1200	1.430	1.979	1.442	0.3758	0.0083	2.5
		900	1.383	1.875	1.406	0.3387	0.0168	2.5
		600	1.337	1.770	1.368	0.3012	0.0229	2.5
		300	1.275	1.648	1.317	0.2600	0.0327	2.5
		0	1.079	1.079	1.052	−0.0245	0.0247	2.5
Direct Flash Liberation	API	0	41.631	5.838	49.684	0.6663	0.1935	0.1
	FVF	0	1.551	1.665	1.403	−0.0221	0.0954	0.1
	GOR	0	878	941.53	626.41	−0.2142	0.2866	0.1
Constant Composition Liberation	Relative	5000	0.9596	0.9283	0.9555	0.0284	0.0043	1
	Oil	4000	0.9716	0.9426	0.9681	0.0262	0.0036	1
	Volume	3000	0.9844	0.9618	0.9826	0.0211	0.0018	1
		2500	0.9916	0.9732	0.9911	0.0180	0.0005	1
		2300	0.9948	0.9782	0.9947	0.0167	0.0001	1
		2200	0.9964	0.9808	0.9966	0.0155	0.0002	1
		2100	0.9981	0.9834	0.9986	0.0142	0.0005	1
		2050	0.9992	0.9848	0.9996	0.0141	0.0004	1
		2015	1.0000	0.9857	1.0024	0.0119	0.0024	1
		2000	1.0031	0.9862	1.0053	0.0147	0.0022	1
		1950	1.0137	0.9876	1.0153	0.0242	0.0016	1
		1900	1.0252	0.9890	1.0260	0.0345	0.0008	1
		1800	1.0512	0.9919	1.0497	0.0550	0.0014	1
		1700	1.0815	0.9949	1.0770	0.0760	0.0041	1
		1500	1.1598	1.0156	1.1455	0.1120	0.0124	1
		1300	1.2716	1.1272	1.2404	0.0890	0.0245	1
		1000	1.5519	1.4072	1.4715	0.0414	0.0518	1
		760	1.9769	1.8362	1.8175	−0.0094	0.0806	1
Reservoir Oil Viscosity Meas.	Oil	5000	0.6589	0.1459	0.7304	0.6700	0.1085	1
	Viscosity	4500	0.6474	0.1417	0.7054	0.6917	0.0895	1
	cp	4000	0.6355	0.1373	0.6795	0.7147	0.0692	1
		3500	0.6260	0.1329	0.8528	0.7450	0.0428	1
		3000	0.6109	0.1282	0.6251	0.7668	0.0233	1
		2500	0.5982	0.1235	0.5965	0.7906	0.0029	1
		2200	0.5907	0.1206	0.5787	0.7756	0.0203	1
		2100	0.5882	0.1196	0.5727	0.7703	0.0264	1
		2050	0.5870	0.1191	0.5697	0.7676	0.0295	1
		2015	0.5861	0.1187	0.5676	0.7658	0.0317	1
		1785	0.5936	0.1200	0.5845	0.7827	0.0153	1
		1500	0.6088	0.1215	0.6080	0.7990	0.0013	1
		1200	0.6348	0.1232	0.6353	0.8050	0.0008	1
		900	0.6900	0.1250	0.6663	0.7845	0.0344	1
		600	0.7720	0.1268	0.7026	0.7459	0.0899	1
		300	0.8540	0.1289	0.7510	0.7284	0.1206	1
		0	0.9360	0.1329	0.9241	0.8453	0.0128	1

*Error Reduction = Error before Regression − Error after Regression

**Error after = (Experimental − Calculated)/Experimental

pressures no miscibility was achieved at pressure less than 4400 psia and the mechanism of recovery seemed to be a condensing/vaporizing mechanism. However, the results do not seem correct because CO_2 should be able to achieve miscibility with most black oils at pressures lower than 3000 psia. The MMP of CO_2 with this oil was calculated using Glaso[2] correlation for pure CO_2 and found 2572 psia. Similar results were achieved for oil 2030R contacted with CO_2 at several different pressures, 2100, 3000 and 4400 psia, as shown in Fig. 20. The MMP of CO_2 with this oil was calculated using Glaso[2] correlation for pure CO_2 and found 2669 psia. The results obtained by EOS may be misleading because the EOS was tuned only with black-oil data and not data for oil mixed with CO_2 that is not available.

VISCOSITY MATCHING OF OILS 1800R AND 2030R

Using the tuned EOS parameters obtained previously, the viscosity of the oil 1800R and 2030 psia were matched using regression on the parameters on the Jossi, Stiel, and Thodos[18] viscosity equation (see Appendix-A). A comparison of the experimental data and the calculated viscosity using the viscosity correlation is shown on Figs. 6 & 12 showing a good match at reservoir conditions above and below bubble point pressure. The final values of the viscosity parameters are shown in Table 1.

MINIMUM MISCIBILITY COMPOSITION DETERMINATION BY THE SLIM TUBE TECHNIQUE

When conducting slim tube experiments, it is essential that any solvent be a single phase at injection conditions. To check this, the pressure-temperature diagrams for solvents with varying amounts of LPG from 10% to 90% were generated. All solvents were found a single phase at the reservoir temperature of 206°F and the injection pressures of 1850 and 2100 psia. Figure 21 represents the pressure-temperature diagram for 40% to 60% LPG solvent.

The two oils were displaced, at reservoir temperature by different solvents made up by blending LPG and Dry Gas,[19,20,21] in a slim tube of 40 feet length, 40.5% porosity and the total pore volume of the system was 99 cc. Figure 22 illustrates the schematic diagram for the slim tube apparatus. Five slim tube experiments were conducted on each oil. For oil 1800R, the injection pressure was 1850 psia while for 2030R the injection pressure was 2100 psia. The first series of experiments were conducted on oil 1800R at 1850 psia by various solvents made up by blending LPG with dry gas in different molar ratios (15%, 25%, 35%, 45% and 55% LPG). The oil recovery in percent was plotted as a function of the LPG% in the solvent as shown in Fig. 23. The oil recovery was calculated when a solvent volume of 1.2 of the total system volume was injected. The intercept of the two straight lines in Fig. 23 shows that the minimum miscibility composition of the solvent was 40% LPG and 60% dry gas for the oil 1800R. In the same manner, the oil 2030R was displaced by solvents of 15%, 20%, 30%, 35% and 40% LPG and the results were plotted in Fig. 24. It was found that a minimum miscibility composition of 35% LPG was required to achieve miscibility with the oil 2030R. From the above experiments, obviously the minimum miscibility composition was over estimated by the EOS for both oils. The slim tube data will be combined with the swelling data when it is ready to re-tune the EOS.

CONCLUSIONS

1. The phase behaviour of both oils 1800R and 2030R were matched using one set of EOS parameters.
2. Using the tuned EOS parameters analysis indicates that miscibility will be achieved for oil 1800R at 1850 psia for LPG ratios of 55% or more. The main mechanism of recovery is a condensing drive.
3. For oil 2030R at 2100 psia miscibility will be achieved via a condensing mechanism for solvent with LPG content of 50% or greater.
4. Minimum miscibility composition for both oils was over estimated using EOS.
5. Any solvent composition will always be single phase at 206°F and 1850 or 2100 psia.
6. Minimum miscibility pressure predicted by EOS for both oils with CO_2 was also over estimated.

ACKNOWLEDGEMENT

Our thanks are expressed to the management of Sirte Oil Company for permission to publish this paper. Thanks are also extended to the management of the Petroleum Research Centre for their support.

APPENDIX A

The viscosity model used in obtaining oil viscosity values is the following

$$[(\eta-\eta^0)\zeta+1]^{0.25} = \text{viscoeff (1)}^* + \text{viscoeff (2)}\ \rho_r + \text{viscoeff (3)}\ \rho_r^2 + \text{viscoeff (4)}\ \rho_r^3 + \text{viscoeff (5)}\ \rho_r^4$$

where

η = phase viscosity, cp
η^0 = low pressure fluid viscosity, cp, calculated

internally from the Jossi, Stiel and Thodos equation, cp

ζ $= T_c^{1/6}\ MW^{1/2}\ P_c^{2/3}$

T_c = fluid pseudo-critical temperature, °K

MW = fluid molecular weight, gm/mol

P_c = fluid pseudo critical pressure, atm

ρr = fluid reduced molar density $= (\rho \times V_C)$

ρ = fluid molar density, kmol/m^3, and

$V_C^{mixvc} = \Sigma(z(i) \times visvc(i)^{mixvc})$

with

$z(i)$ = the mole fracture of component i.

*viscoeff (1–5) for oil 1800R:
1.227600E-01, 2.803680E-02, 7.023960E-02, −4.492087E-02 and 1.119888E-02

*viscoeff (1–5) for oil 2030R:
1.119912E-01, 1.869120E-02, 7.023960E-02, −3.260640E-02 and 7.465920E-03

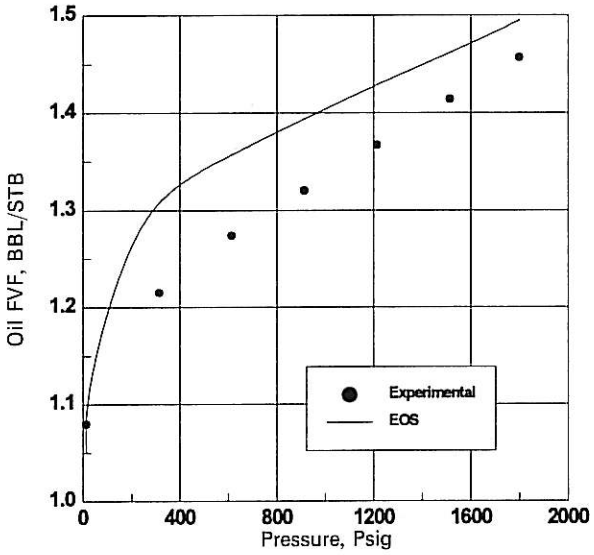


Fig. 1. EOS Match, Oil FVF vs Pressure, Pb = 1800 Psia, Raguba Oil Field – Well No. E40.

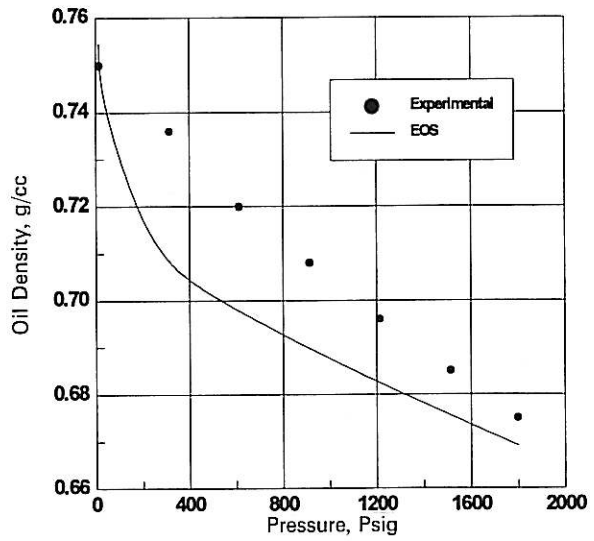


Fig. 2. EOS Match, Oil Density vs Pressure, Pb = 1800 Psia, Raguba Oil Field – Well No. E40.

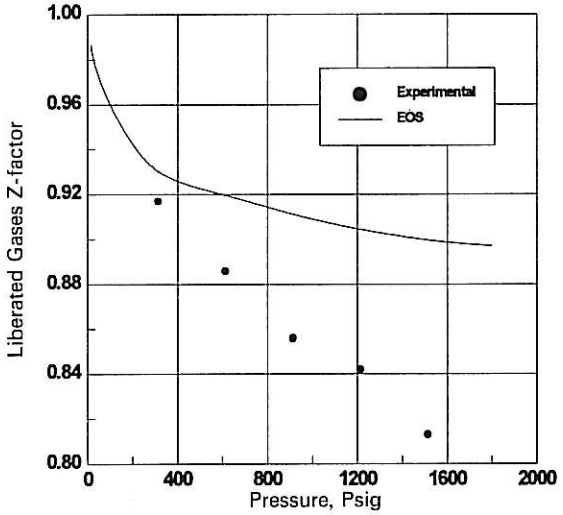


Fig. 3. EOS Match, Liberated Gases Z-factor vs Pressure, Pb = 1800 Psia, Raguba Oil Field – Well No. E40.

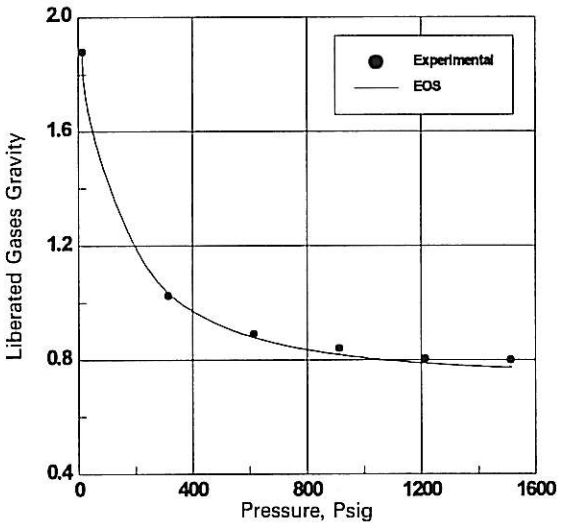


Fig. 4. EOS Match, Liberated Gases Gravity vs Pressure, Pb = 1800 Psia. Raguba Oil Field – Well No. E40.

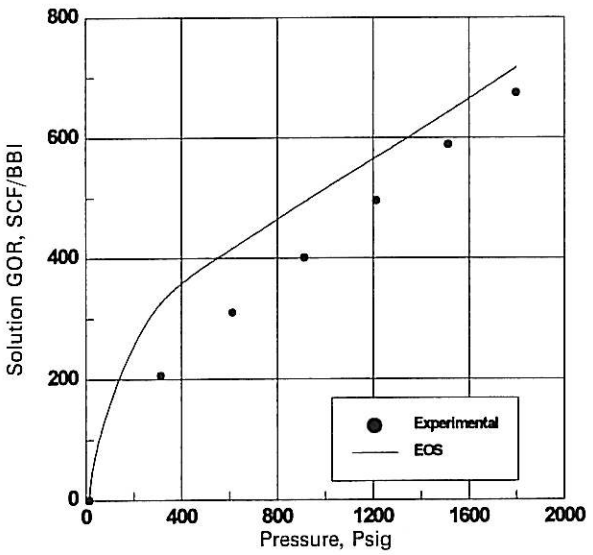


Fig. 5. EOS Match, Solution GOR vs Pressure, Pb = 1800 Psia, Raguba Oil Field – Well No. E40.

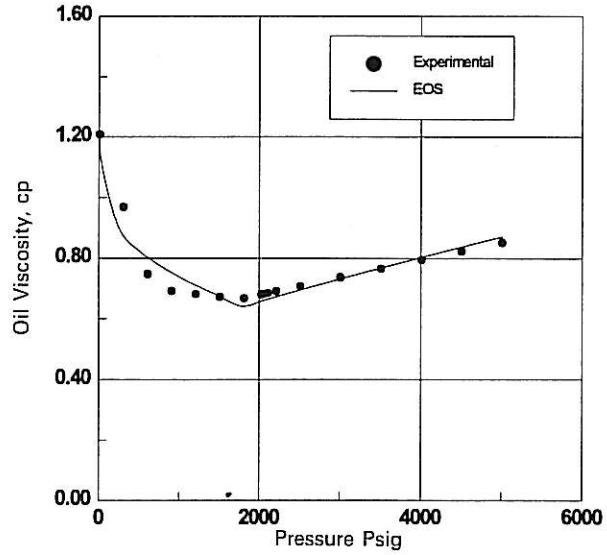


Fig. 6. EOS Match, Oil Viscosity vs Pressure, Pb = 1800 Psia, Raguba Oil Field – Well No. E40.

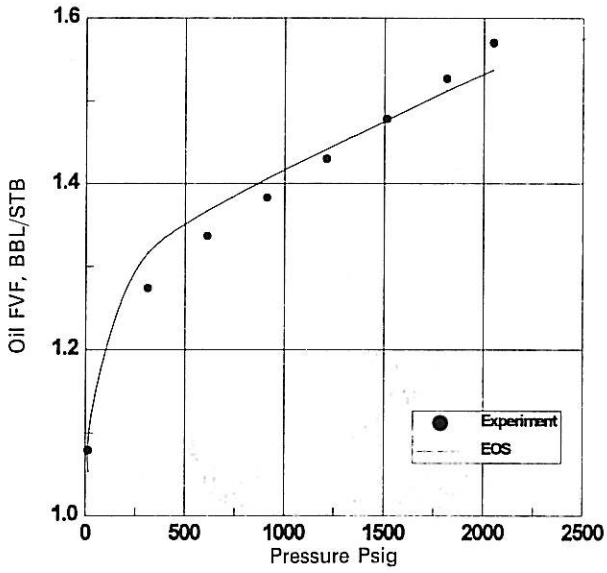


Fig. 7. EOS Match, Oil FVF vs Pressure, PB = 2030 Psia, Raguba Oil Field – Well No. E40.

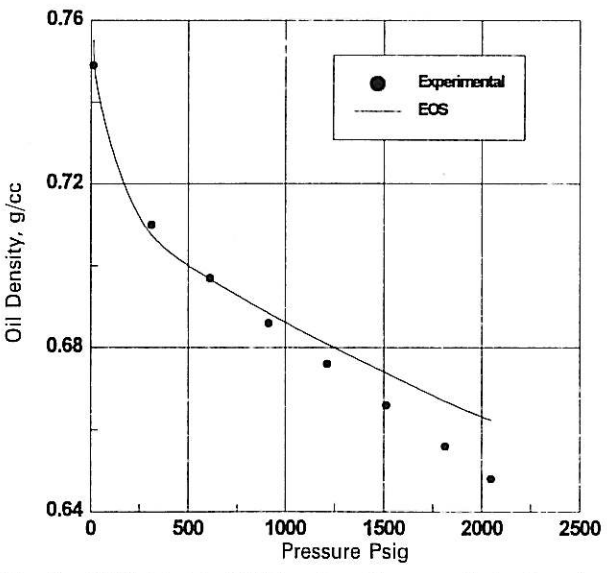


Fig. 8. EOS Match, Oil Densit vs Pressure, Psia, Raguba Oil Field – Well No. E40.

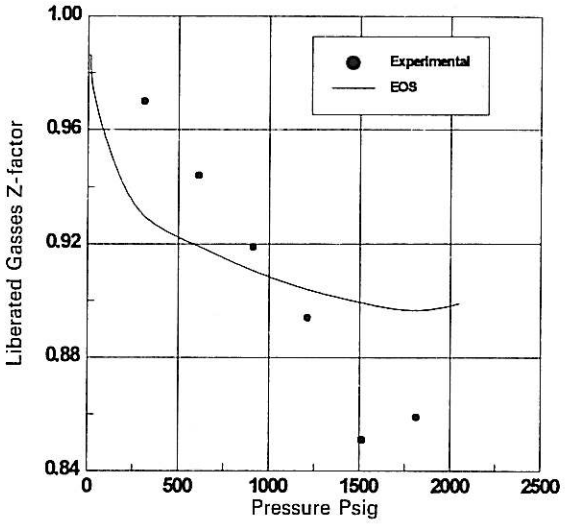


Fig. 9. EOS Match, Liberated Gases Z-factor vs Pressure, Pb = 2030 Psia, Raguba Oil Field – Well No. E40.

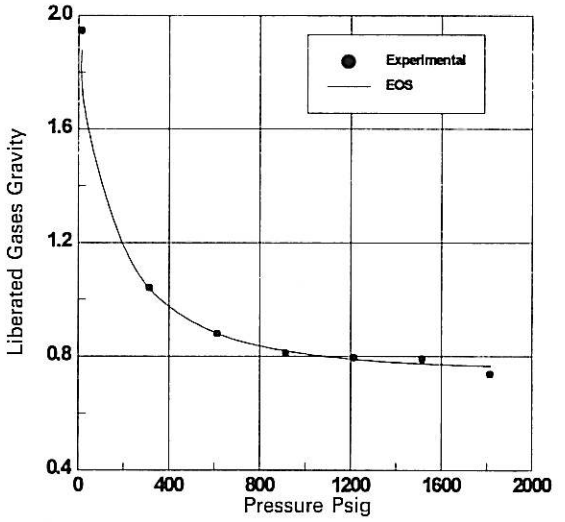


Fig. 10. EOS Match, Liberated Gases Gravity vs Pressure, Pb = 2030 Psia, Raguba Oil Field – Well No. E40.

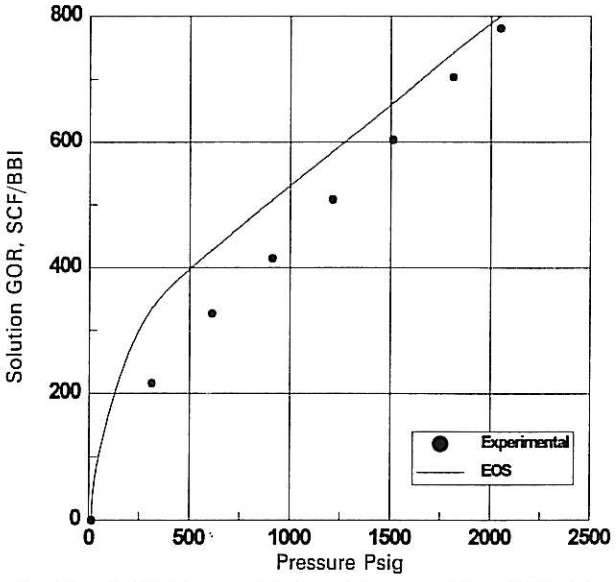


Fig. 11. EOS Match, GOR vs Pressure, Pb = 2030 Psia, Raguba Oil Field – Well No. E40.

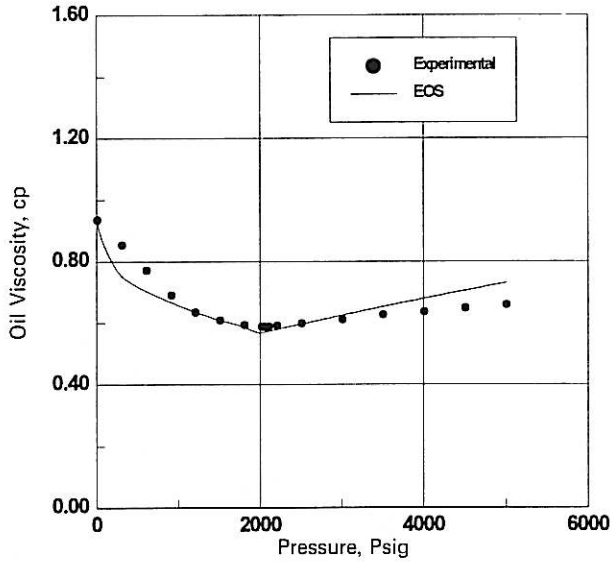


Fig. 12. EOS Match, Oil Viscosity vs Pressure, Pb = 2030 Psia, Raguba Oil Field – Well No. E40.

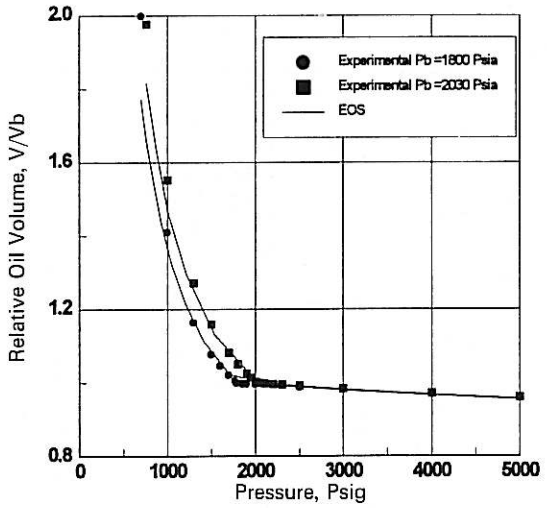


Fig. 13. EOS Match, Relative Oil Volume vs Pressure, Pb = 1800 & 2030 Psia, Raguba Oil Field – Well No. E40.

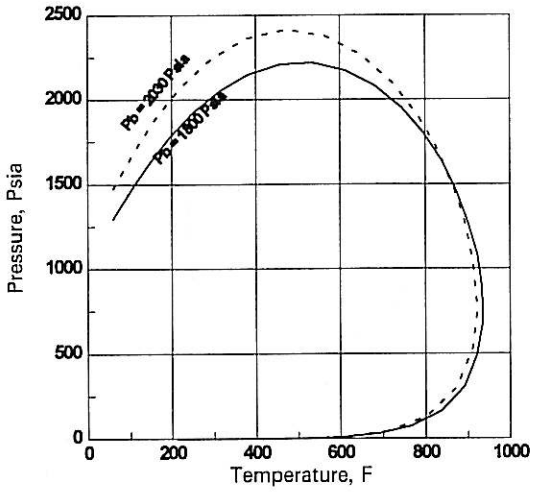


Fig. 14. EOS Generated, Pressure-Temperature Diagram Pb = 1800 & 2030 Psia, Raguba Oil Field – Well No. E40.

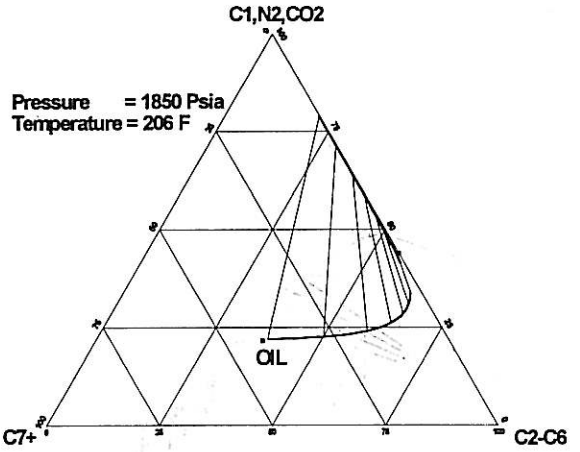


Fig. 15. Ternary Diagram for Solvent LPG/Dry Gas Ratio 55/45 and Resservoir Oil of Pb = 1800 Psia at 206 F. Raguba Oil Field – Well No. E40.

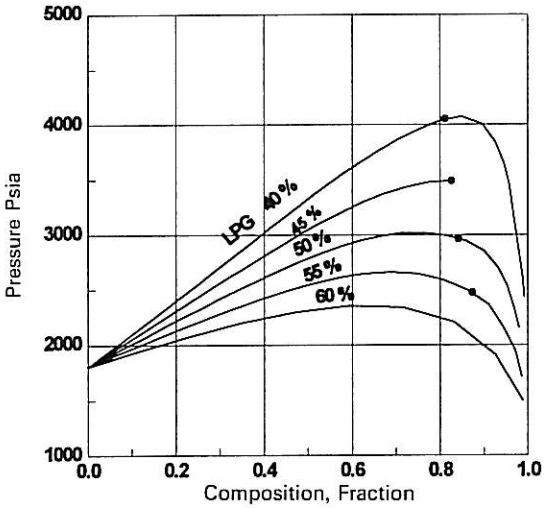


Fig. 16. EOS Generated Pressure-Composition Diagram for Oil 1800R and 5 Mixtures of LPG and Dry Gas, Raguba Oil Field – Well No. E40.

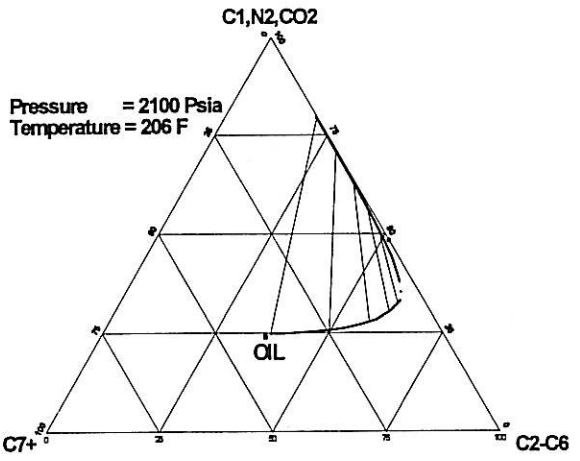


Fig. 17. Temary Diagram for Solvent LPG/Dry Gas Ratio 50/50 and Reservoir Oil of Pb = 2030 Psia at 2030 Psia at 206 F, Raguba Oil Field – Well No. E40.

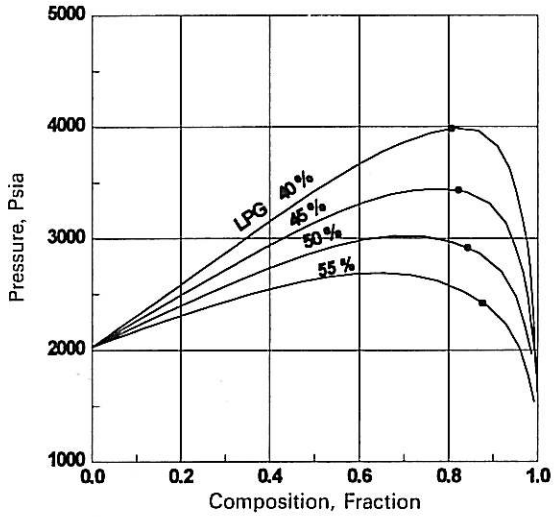


Fig. 18. EOS Generated, Pressure-Composition Diagram for Oil 2030R and 4 Mixtures of LPG and Dry Gas. Raguba Oil Field – Well No. E40.

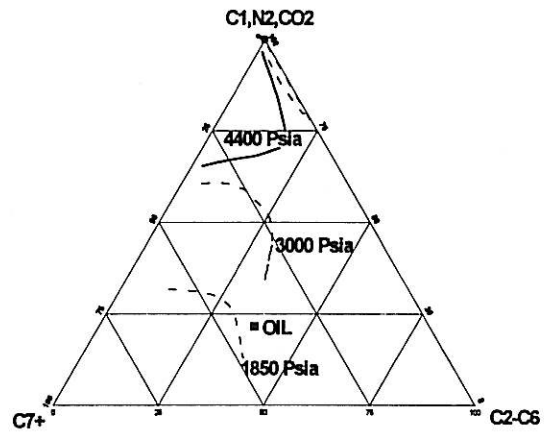


Fig. 19. Ternary Diagram for CO_2 and Reservoir Oil of Pb = 1800 Psia at 206 F, Raguba Oil Field – Well No. E40.

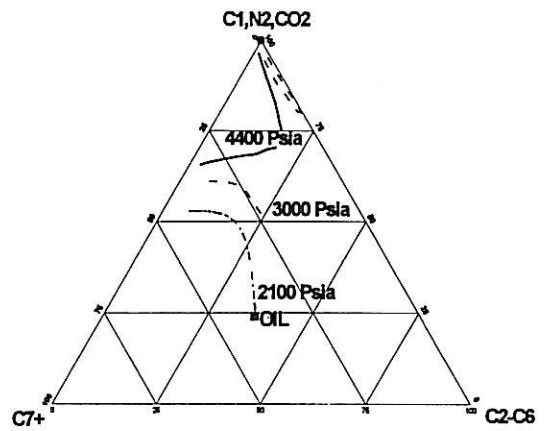


Fig. 20. Ternary Diagram for CO_2 and Reservoir Oil of Pb = 2030 Psia at 206 F, Raguba Oil Field – Well No. E40.

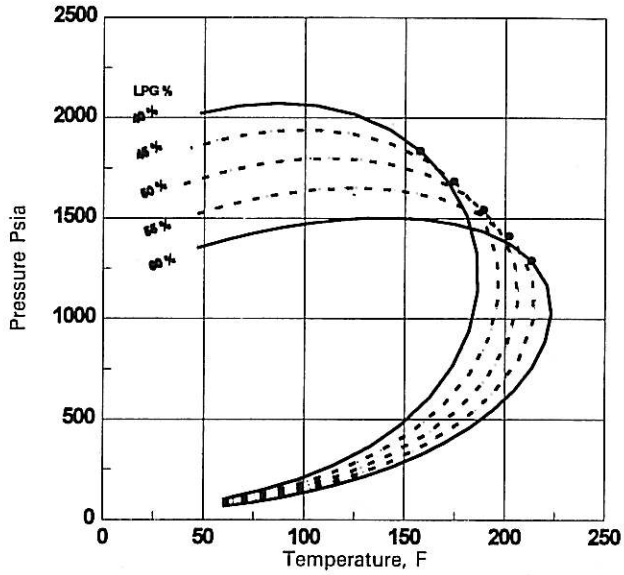


Fig. 21. EOS Generated, Pressure-Temperature Diagram for Different-Mixtures of LPG and Dry Gas, Raguba Oil Field – Well No. E40.

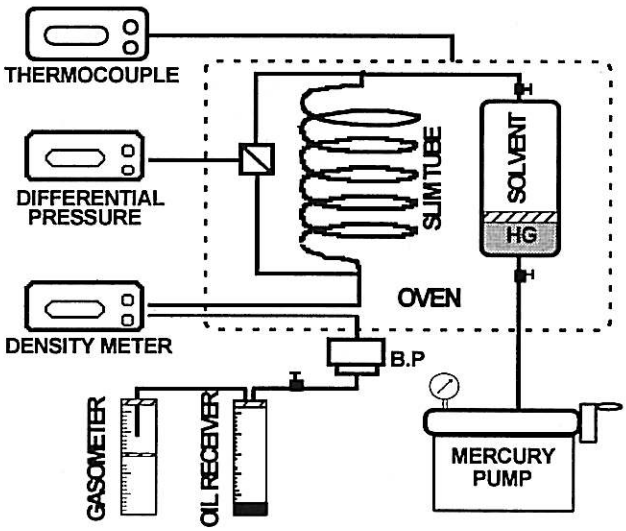


Fig. 22. SLIM TUBE APPARATUS.

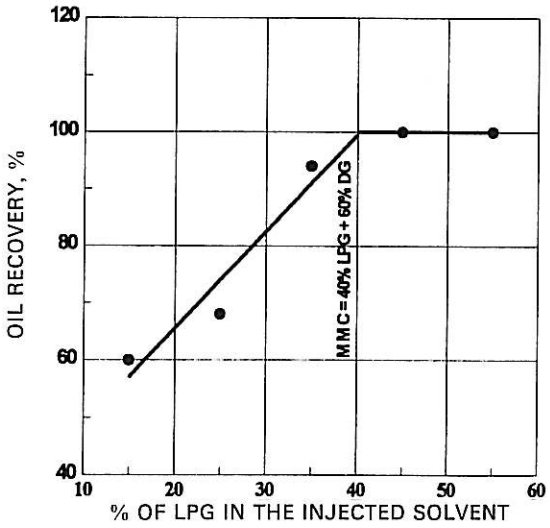


Fig. 23. Oil Recovery as a Function of % LPG in the Injected Solvent, for BPP = 1800 psia, Raguba Oil Field, Well No. E40.

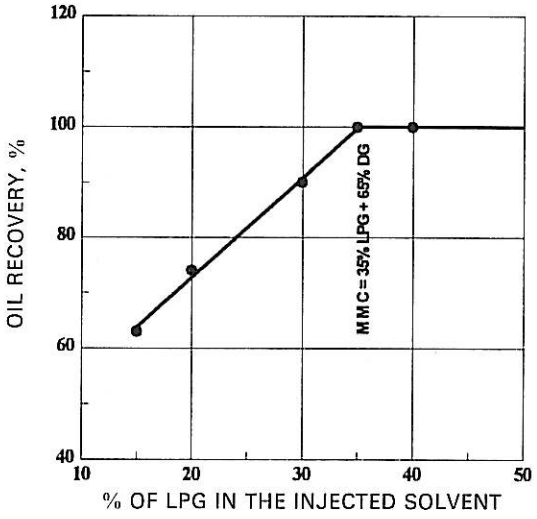


Fig. 24. Oil Recovery as a Function of % LPG in the Injected Solvent, for Oil Sample of BPP = 2030 psia, Raguba Oil Field, Well No. E40.

REFERENCES

[1] Benham, A.L., Dowden, W.E. and Kunzman, W.J., 1960. Miscible fluid displacement prediction of miscibility. *Trans., AIME* **219**, 229–237.

[2] Al-Khafaji, A.H., Al-Dulaimy, S.N. and Al-Doury, M.M., 1989. Correlation for minimum miscibility pressure, hydrocarbon gas-oil systems. *J. Petrol. Res.* **1**, 15–23.

[3] Glaso, O., Dec. 1985. Generalized minimum miscibility pressure correlation. *Soc. Pet. Eng. J.*, 927–934.

[4] Short course prepared and presented by Hycal Research Laboratories LTD, 1990. Design, interpretation and use of experimental laboratory data for miscible flood processes. Second Edition.

[5] Luks, K.D., Turek, E.A. and Baker, L.E., November 1987. Calculation of minimum miscibility pressure. *SPERE*, 501–506.

[6] Thomas, F.B., Bennlon, D.B., Bennlon, D.W., 1991. Recent development in laboratory data sets for determination of miscibility limits, Paper CIM/AOSTRA 91-4 Presented at the CIM/AOSTRA Technical Conference in Banff, (April 21–24) 1–24.

[7] Brigham, W.E., Reed, P.W. and Dew, J.N., March 1961. Experiments on mixing during miscible displacement in porous media, *Soc. Pet. Tech. J.*, 1–8; *Trans., AIME*, 222.

[8] Nutakki, R., Hamoodi, A.N., Li, Y.K., and Nghiem, L.X., 1991. Experimental analysis, modelling, and interpretation of recovery mechanisms in enriched-gas processes, Paper SPE 22634 presented at the 66th annual technical conference and exhibition of the Society of Petroleum Engineering held in Dallas, TX, October 6–9.

[9] Orr, F.M., Jr., Silva, M.K., Lien, C.L. and Pelletier, M.T., April 1982. Laboratory experiments to evaluate field prospects for CO_2 flooding. *J. Pet. Tech.*, 889–898.

[10] DesBrisay, C.L., Gray, J.W. and Spivak, A., August 1975. Miscible flood Performance of the Intisar (D) Field. Libya Arab Republic, *J. Pet. Tech.*, 935–943.

[11] Frazier, G.D. and Todd, M.R., 1982. Alvord (3000-ft Strawn) LPG-design and performance evaluation, Paper SPE/DOE 10692, presented at the SPE/DOE third joint symposium on enhanced oil recovery of the Society of Petroleum Engineering held in Tulsa, Ok, (April 4–7).

[12] Willimanns, C.A., Zana, E.N., and Humphrys, G.E., 1980. Use of Peng-Robinson equation of state to predict hydrocarbon phase behaviour and miscibility of fluid displacement, Paper SPE 8817 presented at the SPE/DOE Enhanced Oil Recovery Symposium, Tulsa, April 20–23.

[13] Benmekkl, E.H., and Mansoori, G.A., May 1988. Minimum miscibility pressure prediction with equation of state, SPERE 559–564.

[14] Enhanced oil recovery project-phase I: PVT studies, Raguba Oil Field, Well No. E40, prepared for Sirte Oil Co., 1994, prepared by Petroleum Research Centre, Tripoli, Libya.

[15] Enhanced oil recovery project-phase II: Equation of state modelling-part (1), Raguba Oil Field, Well No. E40, prepared for Sirte Oil Co., 1994, prepared by Petroleum Research Centre, Tripoli, Libya.

[16] Alston, R.B., Kokolis, G.P. and James, C.F., April 1985. CO_2 minimum miscibility pressure: A correlation for impure CO_2 streams and live oil systems, *Soc. Pet. Tech. J.*, 268–274.

[17] Holum, L.W. and Josendal, V.A., Feb. 1982. Effect of oil composition on miscible-type displacement by carbon dioxide. *Soc. Pet. Tech. J.*, 87–98.

[18] Reid, R.C., Prautsnitz, J.M. and Sherwood, T.K., 1977. *The Properties of Gases and Liquids*, 3rd Edition, McGraw-Hill, New York.

[19] Yarborough, L. and Smith, R., Sept. 1970. Solvent and driving gas compositions for miscible slug displacement. *Soc. Pet. Eng. J.*, 298–310.

[20] Flock, D.L. and Nouar, A., Sept.-October 1984. Parametric analysis on the determination of the minimum miscibility pressure in slim tube displacements. *J. Canadian Pet. Tech.*, 80–88.

[21] Arnold, C.W., Sotne, H.L. and Luffel, D.L., Displacement of oil by rich-gas banks, miscibility processes, SPE reprint series No. 8.